Conducting polypyrrole-coated leathers

Conducting polypyrrole-coated leathers

Fahanwi Asabuwa Ngwabebhoh[a], Tomáš Sáha[a], Jaroslav Stejskal[a,*], Miroslava Trchová[b], Dušan Kopecký[b], Jiří Pfleger[c]

[a]*University Institute, Tomas Bata University in Zlin, 760 01 Zlin, Czech Republic*

[b]*University of Chemistry and Technology, Prague, 166 28 Prague 6, Czech Republic*

[c]*Institute of Macromolecular Chemistry, Academy of Sciences of the Czech Republic, 162 06 Prague 6, Czech Republic*

**Corresponding author. E-mail address: stejskal@utb.cz (J. Stejskal)*

ABSTRACT

Conducting polymers are promising materials applicable as interfaces in various functional materials given they intrinsically possess electronic and ionic conductivity. Herein, a conducting polymer, polypyrrole (PPy) was explored for surface modification of three different leathers via in-situ oxidation of pyrrole in the absence and the presence of two stabilizing polymers, hydroxypropylcellulose and poly(N-vinylpyrrolidone). Colloidal dispersed PPy assemblies were formed with colloidal stabilizers along with PPy-coated leathers and hampered the formation of PPy precipitates that would otherwise contaminate the leather surface. The surface-modified bio-based composites were characterized by $FTIR$ and Raman spectroscopy, and optical and scanning electron microscopy. PPy was deposited on collagen fibers on both sides of the leather. The thickness of the PPy layer varied between 24 and 200 μm. Mechanical properties of the leathers manifested themselves by the decrease in tensile strength and elongation at break after the modification process. Sheet resistances were in the range of 10^0-10^3 $k\Omega/sq$ with the highest values observed for materials modified in the presence of the polymeric stabilizers. Different sheet resistances were obtained for the top and bottom sides of the leathers depending on the surface finishing. Furthermore, the modified leathers were subjected to cyclic bending tests and the variation in their resistivity was studied. The conductivity and electroactivity of the modified materials may serve as guidance for the rational design of intelligent leathers in the footwear, as heating elements, and in energy storage.

Keywords: Polypyrrole, conducting polymer, conducting leather, colloidal dispersions, bending tests sheet resistence

1. Introduction

In recent years, the focus on the use of conductive polymers in electrical devices has greatly paved a path to the development of new class of smart functional materials. These polymers combine good conductivity and electroactivity, and their composites show ease of processing [**1**]. In addition, their ionic conductivity and electrocatalytic activity identifies these polymers suitable for bio-applications [**2-4**]. Among conducting polymers, polypyrrole (PPy) has been explored in the field of materials

science and biomedicine [**5**]. This polymer is easy to synthesize and has excellent environmental stability. The preparation of PPy has been performed in different ways of which the chemical oxidative polymerization has been the most studied. So far, commonly used oxidants of pyrrole to PPy include iron(III) chloride [**6**], ammonium peroxydisulfate [**7**], cerium(IV) sulfate [**8**], and others.

Organic conducting materials enable the development of smart fabrics, which possess desirable properties for application in medicine, fashion design wears (textile and leather) and interior footwear decor that requires electroactivity [**9,10**]. By applying the coating on the surface of various substrates via polymerization of pyrrole, adherent PPy overlayer is obtained. In-situ synthesized PPy coating is physically bound to the surface and withstands even excessive washing. The coated surfaces, however, become often contaminated by a PPy precipitate that is generated outside the coated surface. This is be prevented by the introduction of water-soluble polymers that act as colloidal stabilizers and convert PPy precipitate to colloidal dispersion particles. They have submicrometre size and are easily washed out leaving the PPy-coated substrate clean [**11,12**]. Among water-soluble polymers, poly(N-vinyl-pyrrolidone) (PVP) has often been used to stabilize colloidal dispersions of PPy [**13-15**]. This polymer being hydrophilic in nature and biocompatible has proved to serve as a stabilizing agent in colloidal nanoparticle synthesis [**16,17**]. Other stabilizers used for the stabilization of PPy colloids range from simple water-soluble polymers, such as poly (vinyl methyl ether) [**18**] or cellulose ethers [**19**], to complex tailormade copolymers [**20**]. In the present study, the preparation of colloidal dispersion is not a goal but rather a tool to obtain a high-quality conducting PPy coating.

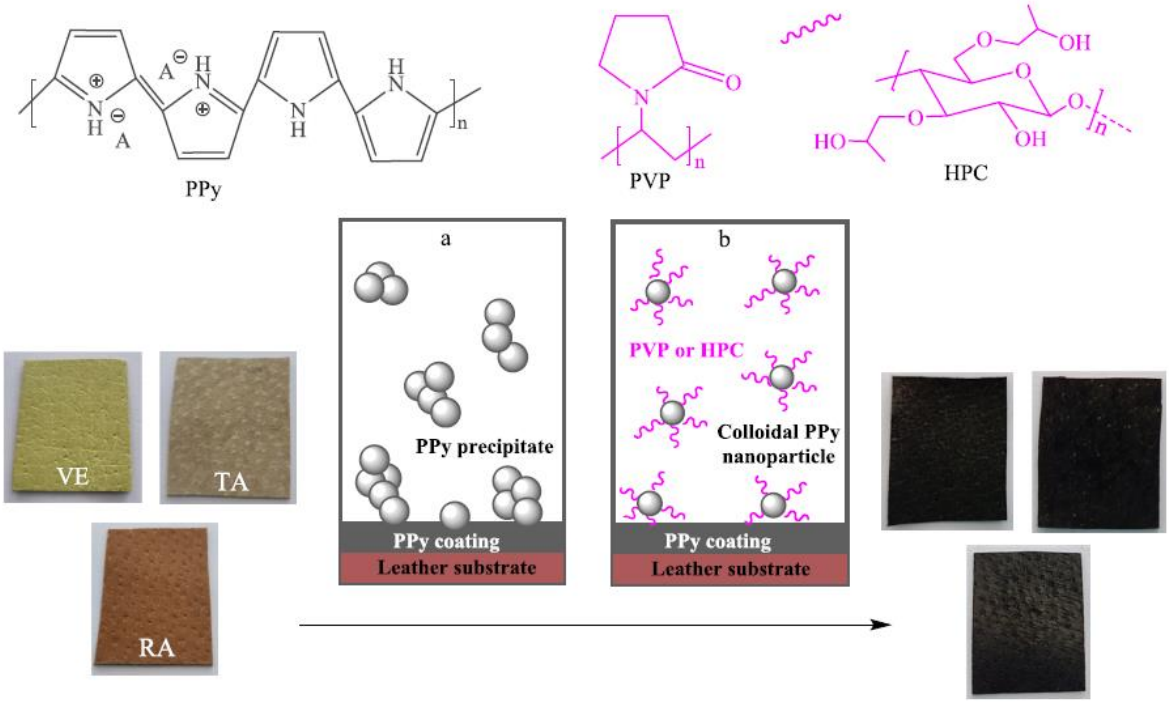

Fig. 1. Schematic representation of (a) leather substrate accompanied by macroscopic PPy precipitate during standard coating and (b) PPy coating in the presence of PVP or HPC, when homogenous dispersion of colloidal nanoparticles is produced. Side images show the leathers before (left) and after PPy coating (right).

Although a number of studies have explored the preparation of PPy as well as its composites with other polymers, there is no systematic study dealing with coating application of PPy on biomaterials, such as leather, for introduction of conductivity and electroactivity for prospective application as smart fabrics. Herein, we introduce the deposition of PPy on different leathers to make them conducting. The routinely synthesized PPy coating is further compared with the deposition of PPy using two

colloidal stabilizers, poly(N-vinylpyrrolidone) and hydrox-ypropylcellulose (HPC). Colloidal PPy dispersions are produced under such conditions and the surface contamination of leather surface with a PPy precipitate is then prevented. Specifically, we have studied the influence of various synthesis protocols using different leathers on the sheet resistance, tensile strength, and stability during bending tests.

2. Experimental

2.1. Leathers

Flat lining pigskin leathers Velur, Tara and Rapid were supplied by the Footwear Research Centre, Tomas Bata University in Zlin, Czech Republic. Velur (VE) is an enhanced grain genuine leather produced on pigskin. This flat lining pigskin leather is a chromium-plated dyed leather, which was modified by graining the pigskin back to increase the evenness of coloring in the area. Increased softness was achieved by higher degree of softening. Tara (TA) is a chrome-plated dyed pigskin leather. The natural face of the leather remains untreated and retains its natural pattern with color irregularity and minor surface damage. This material possesses increased softness achieved by higher degree of softening, accompanied by a loose break of the collar. Rapid sample (RA) is a chromium-plated pigskin leather, dyed with organic dyes containing cutting edge smoothen by ironing.

The leathers had an average thickness 0.5-0.8 mm. They were intended for the use as lining parts of footwear. Their determined tensile strength and elongation at break according to ISO 3376 standard is minimum 12 MPa and 20-80 %, respectively. Slit tear strength in accordance with ISO 3377-2 standard of minimum 35 N and the pH of aqueous extract ranging from 3.5 to 6.0.

2.2. Polypyrrole coating

Pyrrole, iron(III) chloride hexahydrate, hydrochloric acid (37 %), ethanol (98 %), and poly(N-vinylpyrrolidone) (K-90, molecular weight 360,000), were supplied by Sigma Aldrich and hydroxypropylcellulose (Klucel GF) was from Aqualon company. All chemicals were used as delivered without further purification. The coating of VE, TA and RA leathers of dimensions 15 × 10 cm^2 was performed based on three different formulations:

(1) For simple PPy coating, leathers without any pretreatment were immersed in freshly prepared aqueous mixture containing equal 50 mL volumes of 0.1 M pyrrole and 0.25 M iron(III) chloride hexahydrate. The reaction medium thus contained final concentrations of 0.05 M pyrrole (3.35 g L^{-1}) and 0.125 M iron(III) chloride hexahydrate (33.8 g L^{-1}). In-situ polymerization of pyrrole occurred immediately and the reaction mixture darkened. The formation of PPy was completed within a few minutes but the leather substrates were left in the reaction mixture at room temperature for 30 min. The PPy-coated leathers were then removed, repeatedly suspended in 0.1 M hydrochloric acid to remove adhering PPy precipitate, residual reactants, and any byproducts formed in the aqueous phase. Subsequently, the PPy-coated leathers were rinsed repeatedly with ethanol until no coloration of the solvent was observed, and dried in open air overnight. The samples were coded as X/PPy where $X = VE$, TA or RA stands for the individual leathers.

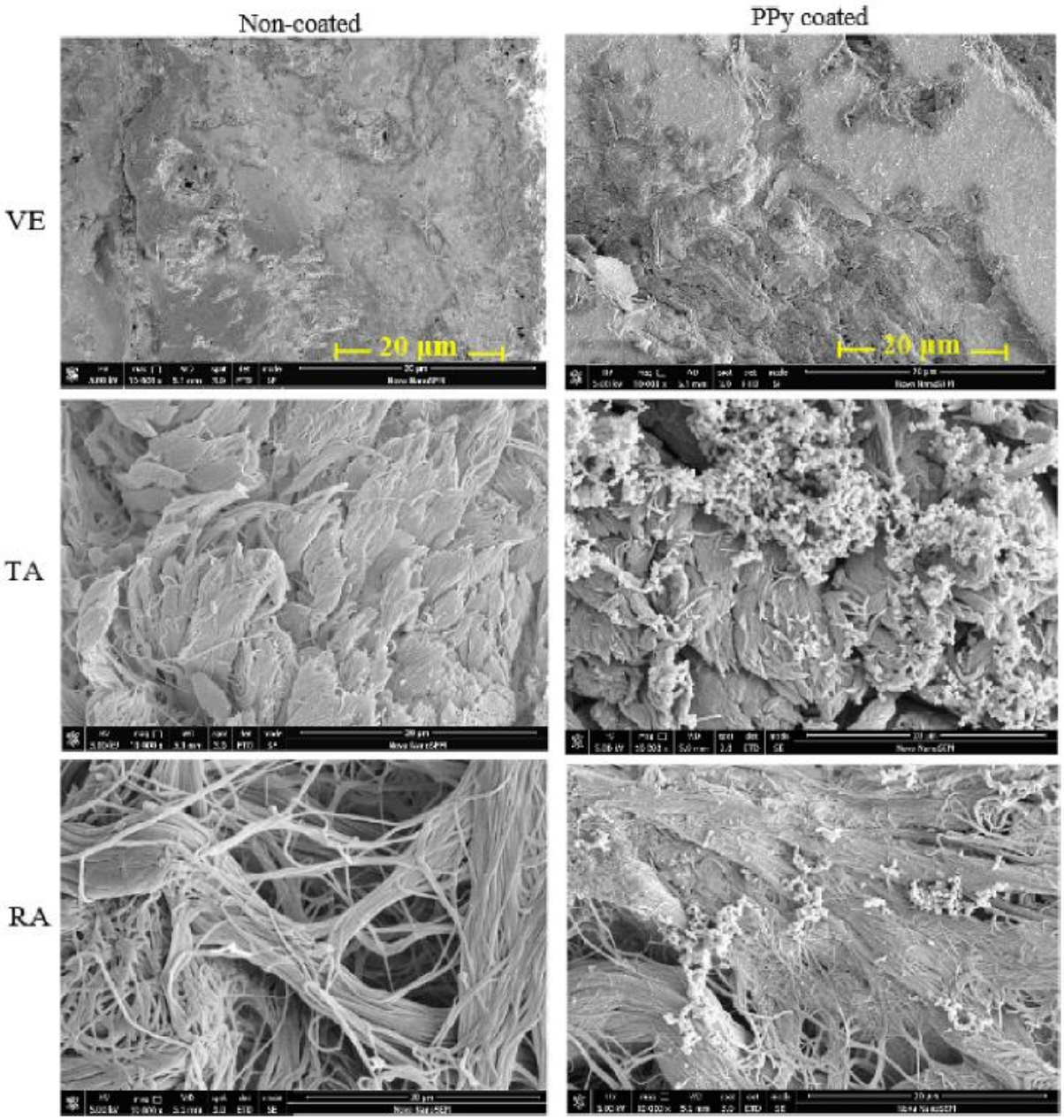

Fig. 2. Surface morphology images of original (left) and PPy-coated (right) VE, TA, and RA leathers.

(2) Polypyrrole-coating in the presence of poly(N-vinylpyrrolidone) ($PPy - PVP$) was produced via in-situ colloidal dispersion protocol. Under such conditions, the formation of a PPy colloid accompanies the PPy-coated substrate. Initially, 0.1 M pyrrole was dissolved in 50 mL of 4 wt% PVP aqueous solution followed by mixing with 50 mL of 0.25 M solution of iron(III) chloride hexahydrate. The final reaction mixture thus contained 0.05 M pyrrole, 0.125 M iron(III) chloride hexahydrate and 2 wt% PVP (20 g L^{-1}). Leathers pretreated with PVP solution were quickly immersed in the freshly prepared reaction mixture and allowed for 30 min for PPy coating to occur. After the coating process was complete, the leather substrates were removed, suspended in 0.1 M hydrochloric acid, rinsed severally with ethanol, and dried in open air overnight. The prepared coated samples were labelled similarly as $X/PPy - PVP$ where $X = VE, TA$ or RA.

(3) Polypyrrole coating in the presence of hydroxypropylcellulose ($PPy - HPC$) was carried out as above. Only in this case, HPC was used as the dispersion stabilizing agent instead of PVP. The coated samples were denoted as $X/PPy - HPC$ where $X = VE, TA$ or RA.

2.3. Optical and scanning electron microscopy

In order to determine the thickness of leather samples and coated conductive layers, a cross-sectional visualization was carried out in diffuse light mode with an optical microscope (Leica DVM2500) with a digital camera. Light from an incandescent bulb was focused onto the samples through a condenser lens and the images were visualized at 100× magnification. The line tool in the Leica software was used to measure the thickness of the dark conducting layers in the optical microscopic images. A random series of 5 measurements was taken on both sides of each material where the PPy layer was clearly visible.

Scanning electron microscopy as performed using a Nova NanoSEM electron microscope (FEI, Brno, Czech Republic) to observe the surface morphology of the original and coated leather samples at different magnifications. Before analysis, the samples were gold sputter-coated with a JEOL JFC 1300 Auto Fine coater.

2.4. Fourier-transform infrared and Raman spectroscopy

$FTIR$ spectra of the original and PPy-coated leathers were analyzed using a Nicolet 6700 spectrometer (Thermo-Nicolet, USA) equipped with reflective ATR extension GladiATR (PIKE Technologies, USA) with a diamond crystal. Spectra were recorded in the 4000-400 cm^{-1} region with a deuterated L-alanine doped triglycine sulfate detector at resolution 4 cm^{-1}, 64 scans and Happ-Genzel apodization.

Raman spectra were collected using a Thermo Scientific DXR Raman microscope equipped with 785 nm line laser. The spot size of the laser was focused by 50× objective. The scattered light was analyzed by a spectrograph with holographic grating 1200 lines/mm, and a pinhole width of 50 μm. The acquisition time was 10s with 10 repetitions.

2.5. Mechanical properties

Tensile testing was conducted based on ISO 3376 standard using an Instron 5567 (Instron, USA) with a static load cell of 3 kN and a crosshead speed of 20 mm min^{-1} at room temperature, ≈25 °C. Prior to testing, five test pieces were cut in accordance with ISO 2419. Using Vernier scale, the width of each test piece was measured to the nearest 0.1 mm at three positions on the grain and flesh side. The thickness of each test piece was also measured as specified by ISO 2589 protocol at three different positions and the average value recorded. The clamp jaws of the tensile testing apparatus was set at 50 ± 1 mm and a pre-test was performed to determine the maximum force. The tensile strength and elongation at break of the test samples were then measured and the values recorded.

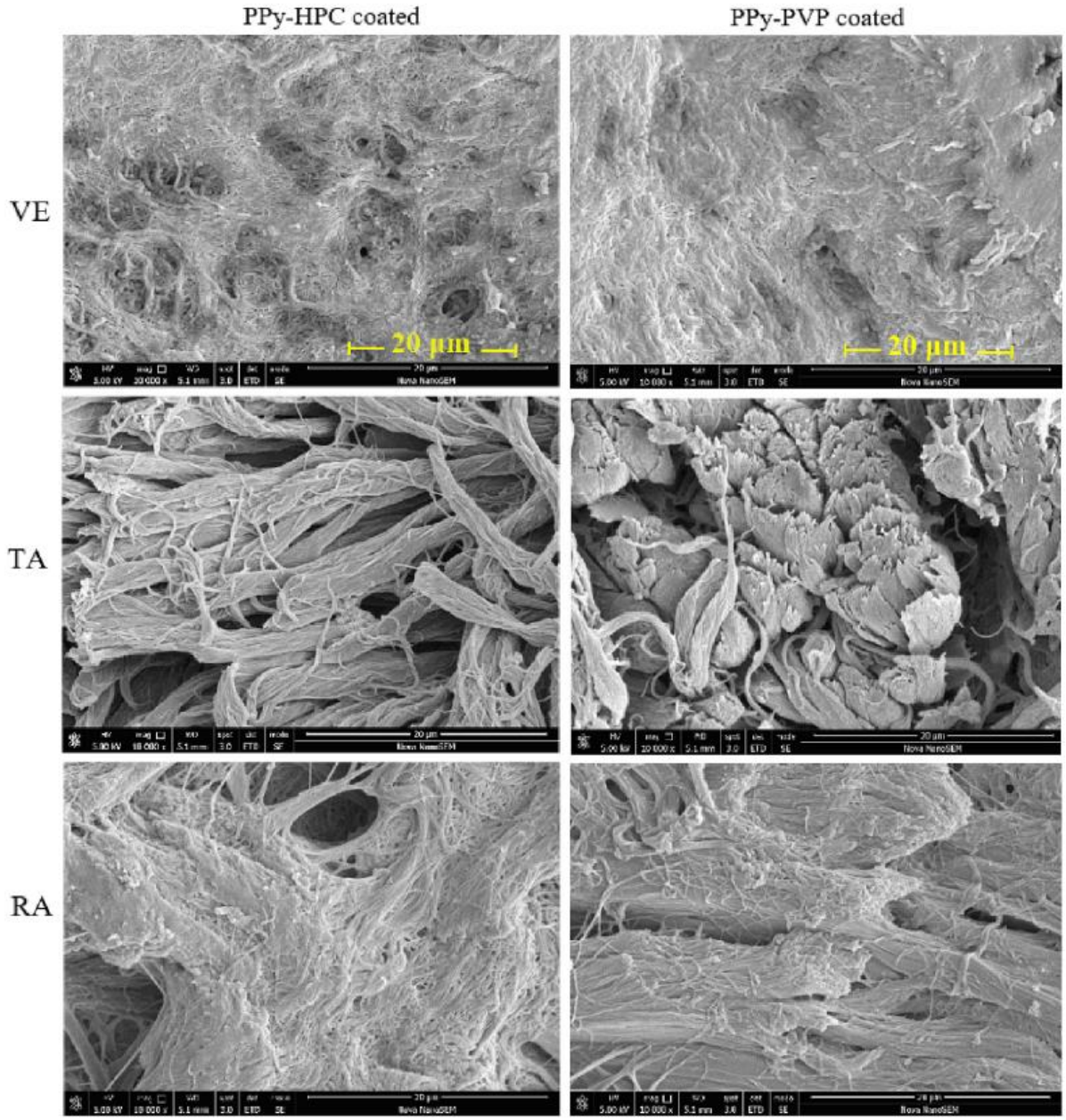

Fig. 3. Surface morphology images of $PPy-HPC$ (left) and $PPy-PVP$-coated (right) VE, TA and RA leathers.

2.6. Cyclic bending

Samples of PPy-coated leathers were subjected to repeated tension or pressure on a purpose-made apparatus for testing of electromechanical properties [**17**]. A PC-controlled servo-motor bended samples under angle a with set duration and number of cycles. DC electrical resistance of samples was acquired during bending and subsequently processed as

curves of sample resistance in non-bended and bended states, R_{OFF} and .R_{ON}, respectively. A relative resistance change in nth cycle was calculated as $|R_{rel(n)} - = [(R_{ON(n)} - R_{OFF(n)}) / R_{OFF(n)}] \times 100$.

Samples of were tested in both tension and pressure modes, under bending angles α = 30° and 45°. Altogether 500 cycles have been used for comparative tests, each cycle lasted 20 s. In the tension mode

samples were subjected to strain caused by sample elongation and in the pressure mode to strain caused by sample compression.

Table 1 Conducting layer thickness of the different coated leathers.

Leathers	PPy layer (μm)		Leather thickness (μm)
	Top	Bottom	
VE	0	0	540 ± 49
VE/PPy	206 ± 15	146 ± 16	621 ± 27
VE/PPy-HPC	220 ± 26	154 ± 11	613 ± 20
VE/PPy-PVP	185 ± 20	178 ± 20	605 ± 7
TA	0	0	585 ± 18
TA/PPy	63 ± 5	47 ± 4	734 ± 17
TA/PPy-HPC	134 ± 7	118 ± 10	602 ± 30
TA/PPy-PVP	29 ± 3	24 ± 3	651 ± 24
RA	0	0	502 ± 10
RA/PPy	91 ± 13	59 ± 12	643 ± 20
RA/PPy-HPC	101 ± 11	92 ± 2	538 ± 17
RA/PPy-PVP	117 ± 12	29 ± 4	632 ± 13

2.7. Sheet resistence

The sheet resistance was determined using a linear four-probe method with Jandel cylindrical probe, with current probes connected to a Keithley 230 power supply (Keithley Instruments, USA) and Keithley 196 multimeter as a current source and potential probes connected to a Keithley 181 nanovoltmeter for the voltage-drop measurement. The current was reduced to keep the dissipated energy below 50 μW. The Jandel probe was placed at three places within the inner rectangular area of the 13 × (17-35) mm^2 size. The sheet resistance was calculated from the linear part of the I-V characteristics according to the formula R_{SR} = 4.53 x U / I, assuming that the thickness of the conducting layer was much smaller than the distance between the probes.

3. Results and discussion

3.1. Leather coating with polypyrrole

The polymerization of pyrrole via oxidation in aqueous medium to produce PPy was performed. Any material in contact with the aqueous reaction mixture, herein collagen fibers constituting leather samples, becomes coated with a thin submicrometre layer of PPy [**17,21,22**] (**Fig. 2**). The oxidation of pyrrole starts with the formation of oligomers. They adsorb at available solid interfaces, collagen fibers, and promote the growth of PPy chains that form organized brush-like film at the fibers surface. The interaction between the collagen and PPy is based on adsorption and hydrophobic interactions. The polypyrrole-coated leathers cannot be regarded as simple blends of a biopolymer and a conducting polymer that could be described by interactions in term of the thermodynamic approach [**23,24**].

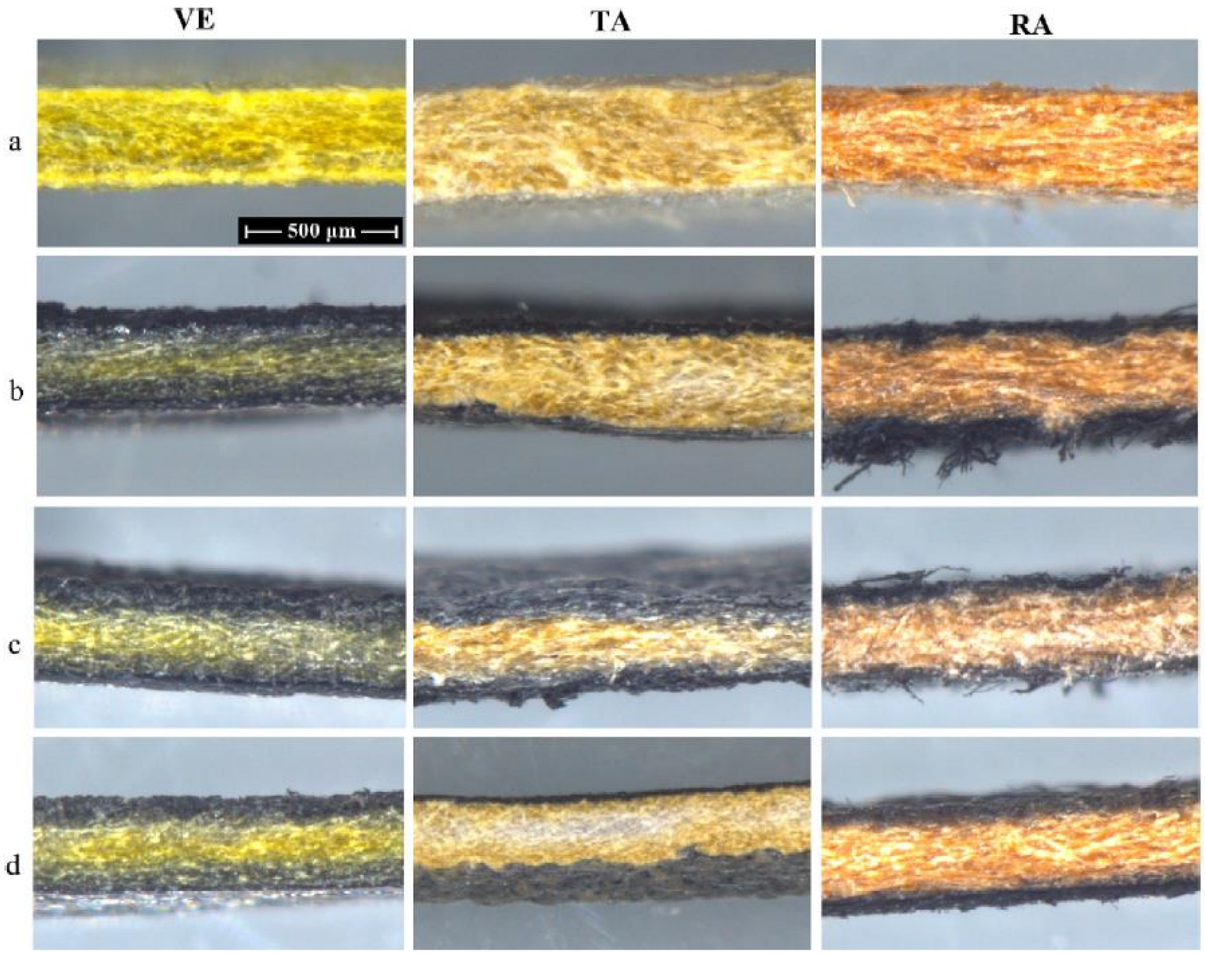

Fig. 4. Cross-sectional optical microscopic images of (a) original, (b) PPy, (c) $PPy - HPC$, and (d) $PPy - PVP$-coated leathers VE, TA and RA showing the dark conducting layers.

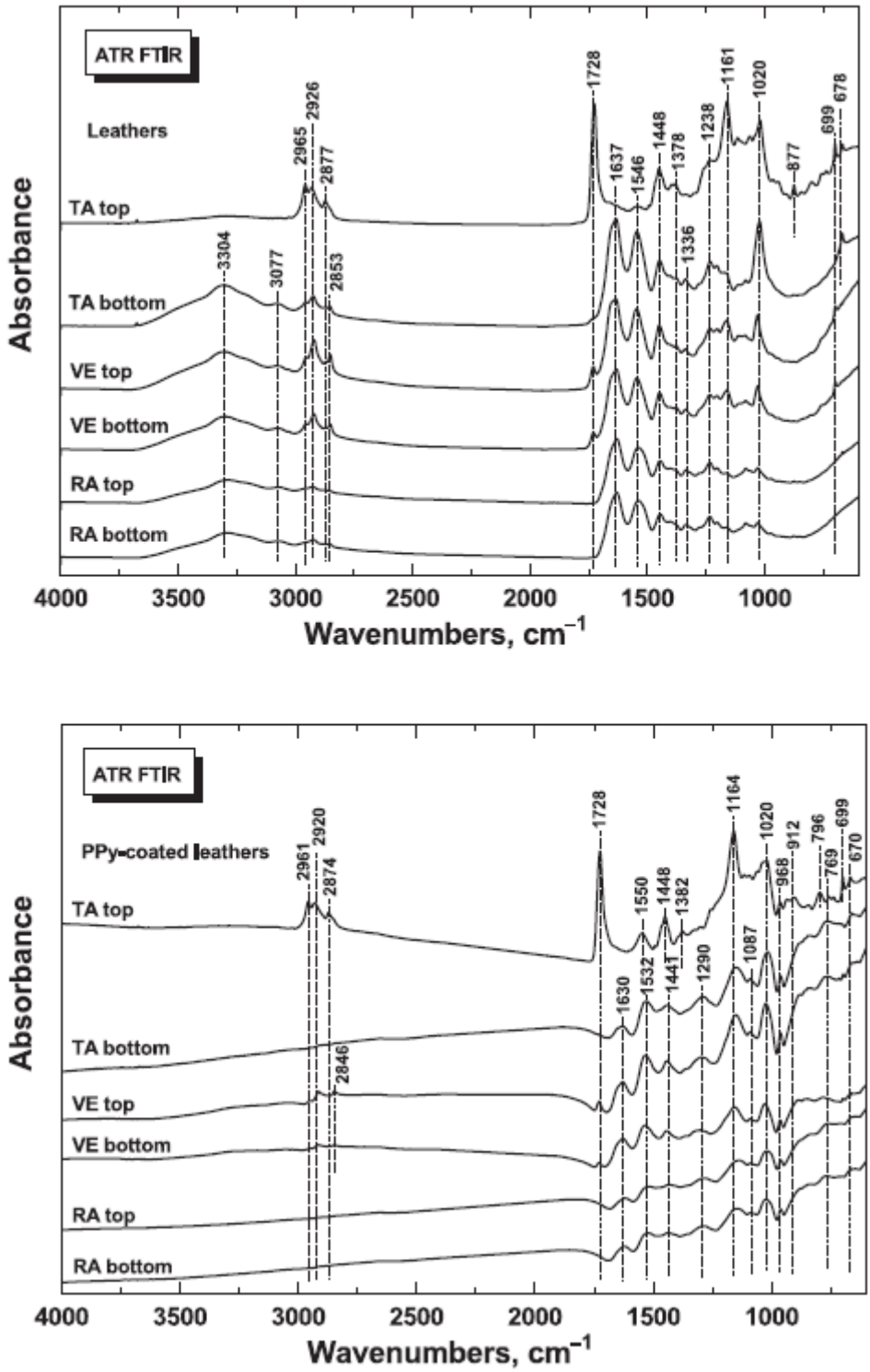

Fig. 5. $ATR\ FTIR$ spectra of original leathers (top) and leathers coated with polypyrrole (bottom) taken on top and bottom sides.

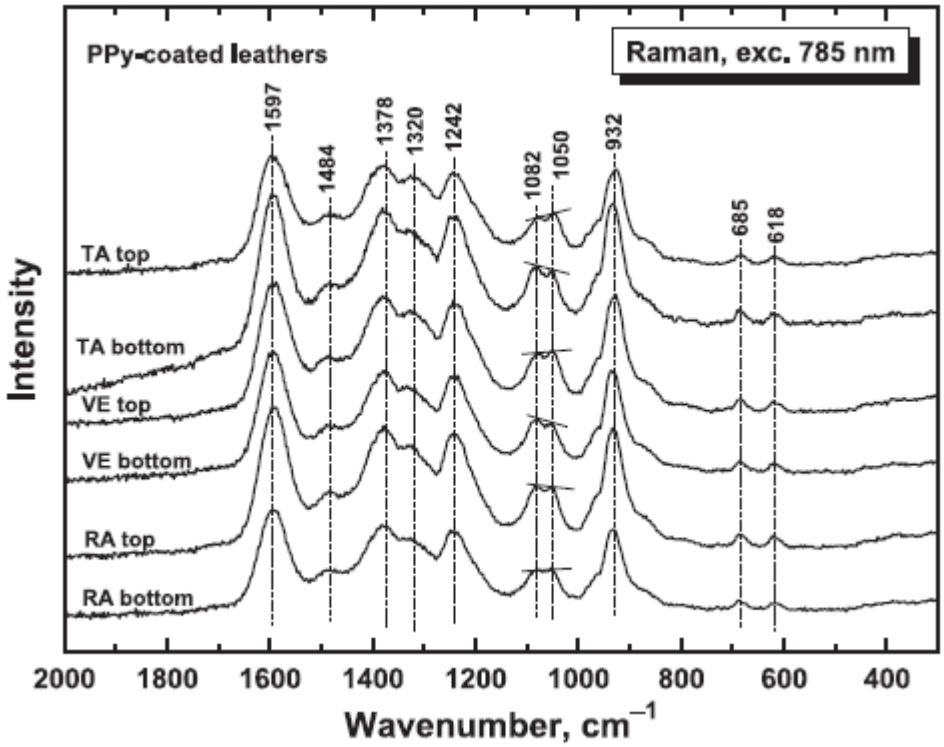

Fig. 6. Raman spectra of leathers coated with polypyrrole taken on top and bottom sides.

Table 2 Mechanical parameters of the original and coated leathers.

Leathers	Breaking load (N)	Tensile strength (MPa)	Elongation at break (%)
VE	43.8 ± 2.7	15.4 ± 0.9	39.3 ± 1.0
VE/PPy	13.7 ± 2.8	4.4 ± 0.5	43.3 ± 1.3
VE/PPy-HPC	20.3 ± 3.4	6.6 ± 0.8	36.0 ± 0.7
VE/PPy-PVP	16.2 ± 1.6	5.8 ± 0.2	30.1 ± 1.0
TA	34.2 ± 2.8	12.1 ± 0.8	26.8 ± 1.1
TA/PPy	7.0 ± 0.9	1.9 ± 0.2	44.5 ± 2.8
TA/PPy-HPC	31.0 ± 3.7	7.6 ± 0.6	50.9 ± 3.3
TA/PPy-PVP	70.6 ± 5.3	16.6 ± 3.7	53.3 ± 1.5
RA	95.8 ± 8.3	26.6 ± 2.3	48.9 ± 3.9
RA/PPy	33.4 ± 3.1	10.8 ± 1.9	38.3 ± 0.7
RA/PPy-HPC	88.8 ± 9.2	26.1 ± 2.5	46.9 ± 1.4
RA/PPy-PVP	64.4 ± 3.6	18.9 ± 1.1	57.3 ± 1.5

In the absence of any additive, globular PPy particles are also formed in the aqueous solution surrounding the leather materials by selfassembly of PPy chains [**25**]. They adhere to the PPy film growing on fibers (**Fig. 1**a and b). The formation of PPy precipitate in the aqueous medium cannot be

completely suppressed [**25**], unless the reaction mixture contains a water-soluble polymer stabilizer, such as PVP or HPC. Under such conditions, submicrometre colloidal particles, PPy/PVP or PPy/HPC, are produced instead of a macroscopic precipitate (**Fig. 1**b). They are easily washed out and do not significantly contaminate PPy coating of the individual leather fibers.

3.2. Surface morphology

SEM micrographs reveal the fibrous structure of leathers. There was a distinctive difference in the surface morphology of the uncoated and PPy-coated leather (**Fig. 2**). As observed, PPy-coated materials display the presence of some globular PPy aggregates with non-uniform distribution (**Fig. 2**). They are easily mechanically removed and the PPy-coated surfaces are regarded as dirty.

The polymerization of pyrrole in the presence of different stabilizers (**Fig. 3**) produced smooth and uniform PPy coating on leather surfaces. This is attributed to the even and thin layer adherence of PPy overlayer grown on the leather fibers when immersed in the coating medium containing PVP or HPC stabilizers. If the PPy-coated surface is subjected to a peel-off test with an adhesive tape, no conducting polymer is separated [**17**].

3.3. Coating thickness

The thickness of the PPy coating on the individual fibers is at submicrometre level [**25**]. The thickness of conducting phase constituted by many coated fibers is given by the penetration deepness of the reaction mixture into leather body. The latter parameter is important to comprehend the electrical properties (**Table 1**). The thickness of conducting phase was determined from the dark areas visible by crosssection optical imaging (**Fig. 4**). This parameter significantly varied for the top and bottom sides due to their different porosity. It has a significant impact on the surface resistance and mechanical properties. In general, the thickness is predetermined following the material hy-drophilicity and consequent penetrability of the aqueous reaction mixture into the inner structure of the leather. The thickness of conducting phase could be increased by the decrease in reactant concentrations and consequent slowdown of the polymerization rate resulting in longer time allowed for the reaction mixture penetration. It has also been demonstrated that the coatings in the presence of stabilizers, PVP and HPC, are thinner than those prepared in their absence. This may be attributed to the higher viscosity of reaction mixture and reduced penetration to the leather. The irregularities observed on the surfaces can be explained by the roughness of the leather materials, which relates to the finishing process of the leathers. This can be seen on the image of the cross-section where the coating is following the surface structure of leather fabrics.

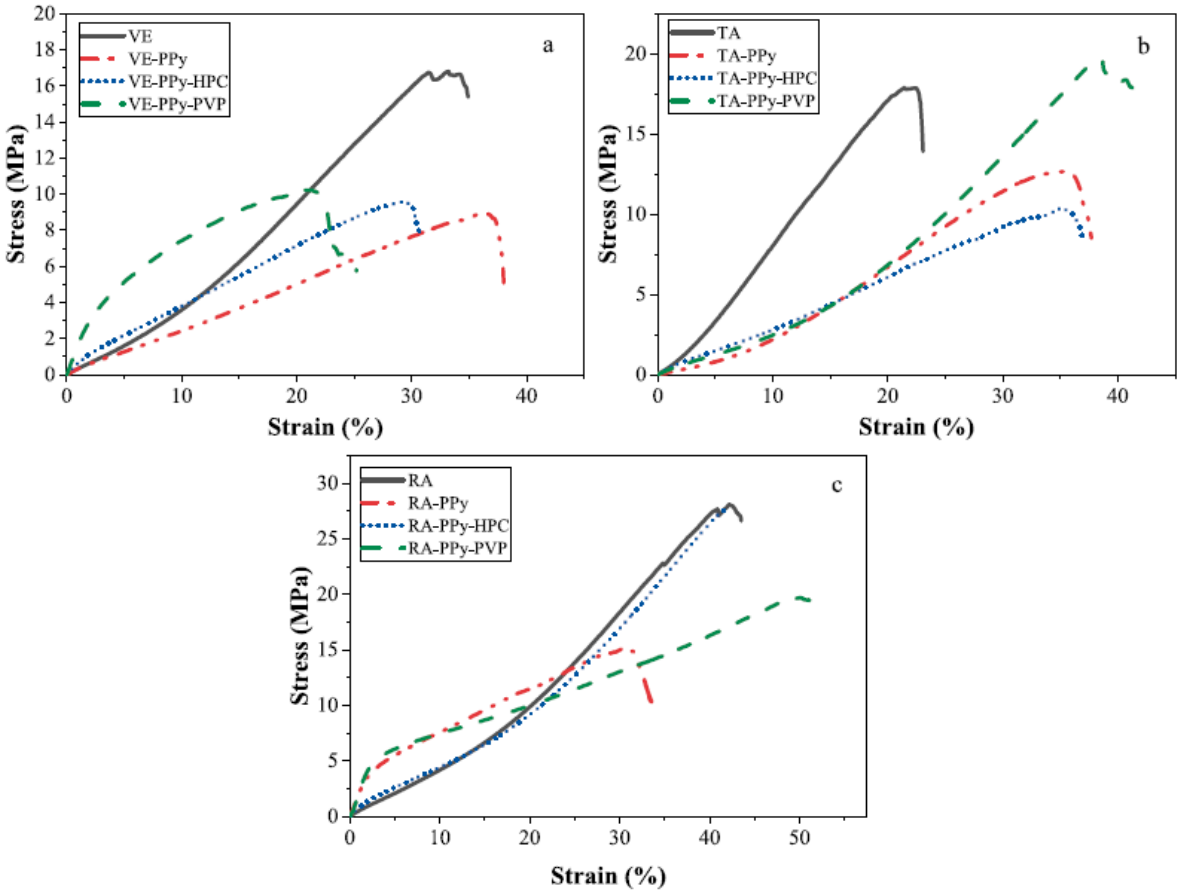

Fig. 7. Stress-strain curves of (a) VE, (b) TA and (c) RA non-coated and PPy-coated leathers.

Table 3 Sheet resistances (kΩ/sq) of the leathers coated with polypyrrole.

Coating	TA		VE		RA	
	Top	Bottom	Top	Bottom	Top	Bottom
PPy	29 ± 5	16 ± 0.3	7 ± 0.8	5 ± 0.2	14 ± 0.4	20 ± 1.2
PPy-HPC	1770 ± 200	4120 ± 850	363 ± 15	750 ± 92	424 ± 170	309 ± 103
PPy-PVP	132 ± 19	580 ± 400	302 ± 20	48 ± 12	374 ± 280	300 ± 49

3.4. FTIR spektra

The major component of leathers is collagen constituted by polypeptide chains. $ATR\ FTIR$ spectra of non-coated leathers (**Fig. 5**a) recorded on bottom side exhibit a broad band from 3700 to 3000 cm^{-1} which corresponds to the stretching vibrations of hydroxyl group overlapped with Amide A band of N—H stretching vibrations with maximum at 3322 cm^{-1} The maxima observed at 3077 (overtone of Amide II band), 2965, 2926, and 2877 cm^{-1} are attributed to the C—H stretching vibrations. In the spectrum of TA from the top site the band of hydroxyl is missing and the bands of C—H stretching vibrations are relatively strong. In the spectra of all leathers measured from the top and bottom site the main bands of Amide I (mainly associated with the C=O stretching vibrations) and the Amide II (results from N—H bending vibrations and from C—N stretching vibrations) are observed at 1637 and

1546 cm^{-1}. These bands are characteristic for poly(N-methyl-acrylamides). The peak at 1448 cm^{-1} (C—H deformation vibration), and the Amide III band (a very complex band depending on the nature of side chains and hydrogen bonding) is situated at about 1238 cm^{-1}. A strong peak situated at 1020 cm^{-1} belongs most probably to the SO_3 group coming from chromium sulfate. This peak is very small in the spectrum of RA sample from top and bottom. In the $ATR\ FTIR$ spectrum of sample TA recorded at the top side, the bands of Amide I and Amide II are missing, it exhibits a strong maximum at 1728 cm^{-1} (C=O stretching vibrations), and it is close to the spectrum of polyacrylate with maxima at 1735 cm^{-1} (C—O stretching vibrations), the peaks at 1452 and 1378 cm^{-1} (C—H deformation vibration), a strong peak at 1164 cm^{-1} (C=O stretching vibrations), and 1109 cm^{-1}. This reveals that the top side of these samples is coated with a synthetic polyacrylate overlayer. $ATR\ FTIR$ spectra of leathers coated with PPy exhibit the main bands of PPy situated at 1630, 1532, 1441, 1290, 1160, 1087, 1020, and 968 cm^{-1} [**21**] (**Fig. 5**b). This proves that leathers are well coated with PPy.

3.5. Raman spektra

Contrary to the infrared spectra, in the Raman spectra of leathers coated with PPy we observe mainly the bands of polypyrrole with local maxima at 1597 cm^{-1} (C=C stretching vibrations of PPy backbone), a maximum at 1484 cm^{-1}, two bands of ring-stretching vibrations at 1378 and 1320 cm^{-1} (the intensity of the latter increases after deprotonation), the band at 1242 cm^{-1} (antisymmetric C—H deformation vibrations), the double peak with local maxima at 1082 and 1050 cm^{-1} (C—H out-of-plane deformation vibrations, the second becomes sharper in case of deprotonation) [**26**] (**Fig. 6**). This is due to the fact, that the energy of the laser excitation wavelength 785 nm is in resonance with the energy of delocalized polarons and bipolarons in polypyrrole salts constituting the coating. As the Raman spectra of neat leather exhibit the strong fluorescence, which is absent in PPy-coated samples, they strongly support the uniform deposition of collagen fibers. In addition, they provide the information about the protonation state of the PPy coatings [**27**], which is essential for electrical conduction.

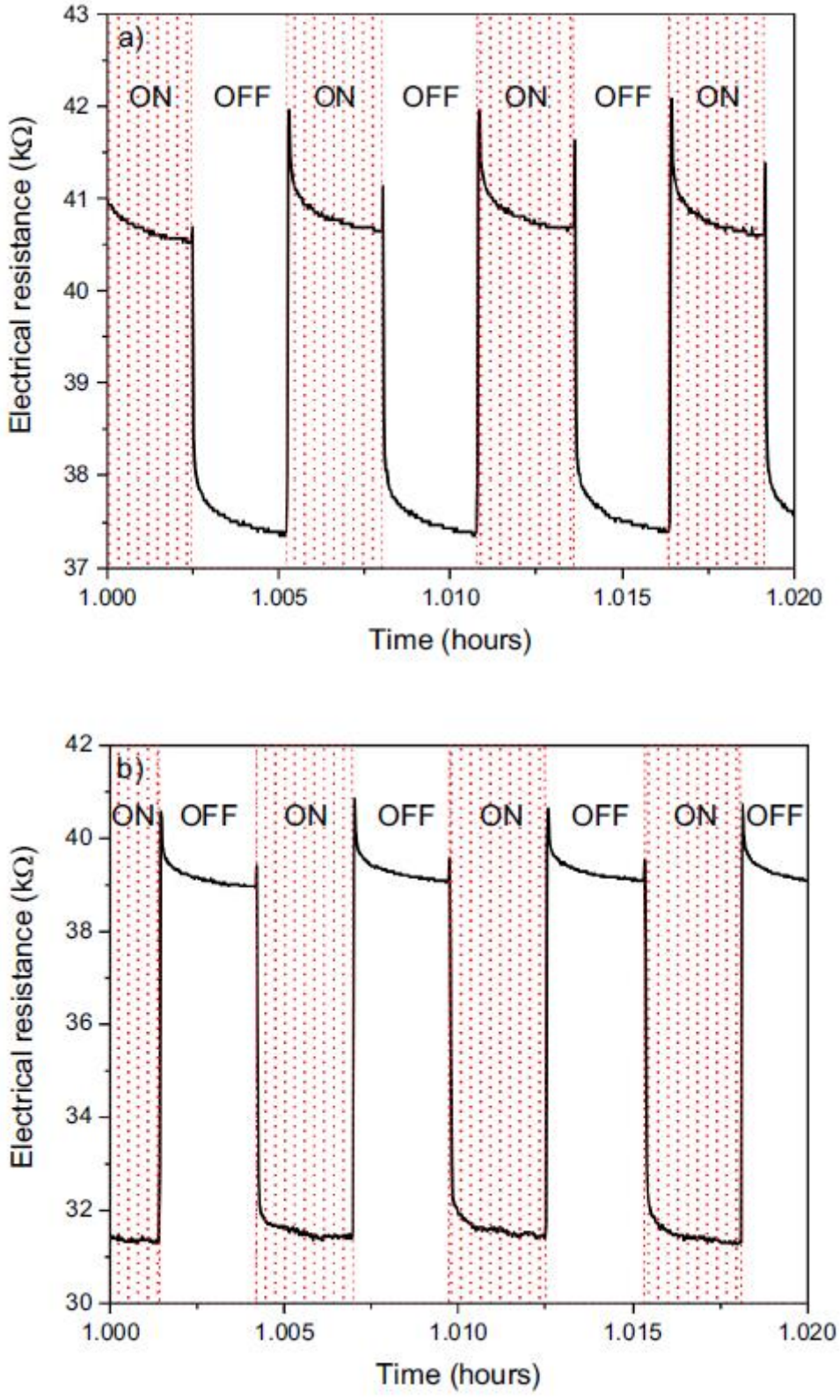

Fig. 8. Cyclic TA/PPy sample bending: a detail of 3 cycles after 1 h of measurement: (a) the tension mode and (b) the compression mode.

3.6. Mechanical properties

Mechanical properties of the PPy-coated leather were investigated (**Table 2**, **Fig. 7**). Breaking load and tensile strength for the coated leather materials decreased ≈50 % when compared to the pristine leather. The elongation at break appears to be in close range to the pristine leathers. In addition, leathers coated in dispersion mode, $PPy - HPC$ and $PPy - PVP$, possess higher mechanical stability than original leathers. Coating of the leather materials with PPy to some extent decreases the strength of the leathers and results in the loss of elasticity. The decrease in strength caused by PPy is counterbalanced by the incorporation of HPC and PVP stabilizers during the coating of the leather materials. In this case, the failure of the materials may be caused by fracture of the interface rather than by fiber pullout from the matrix.

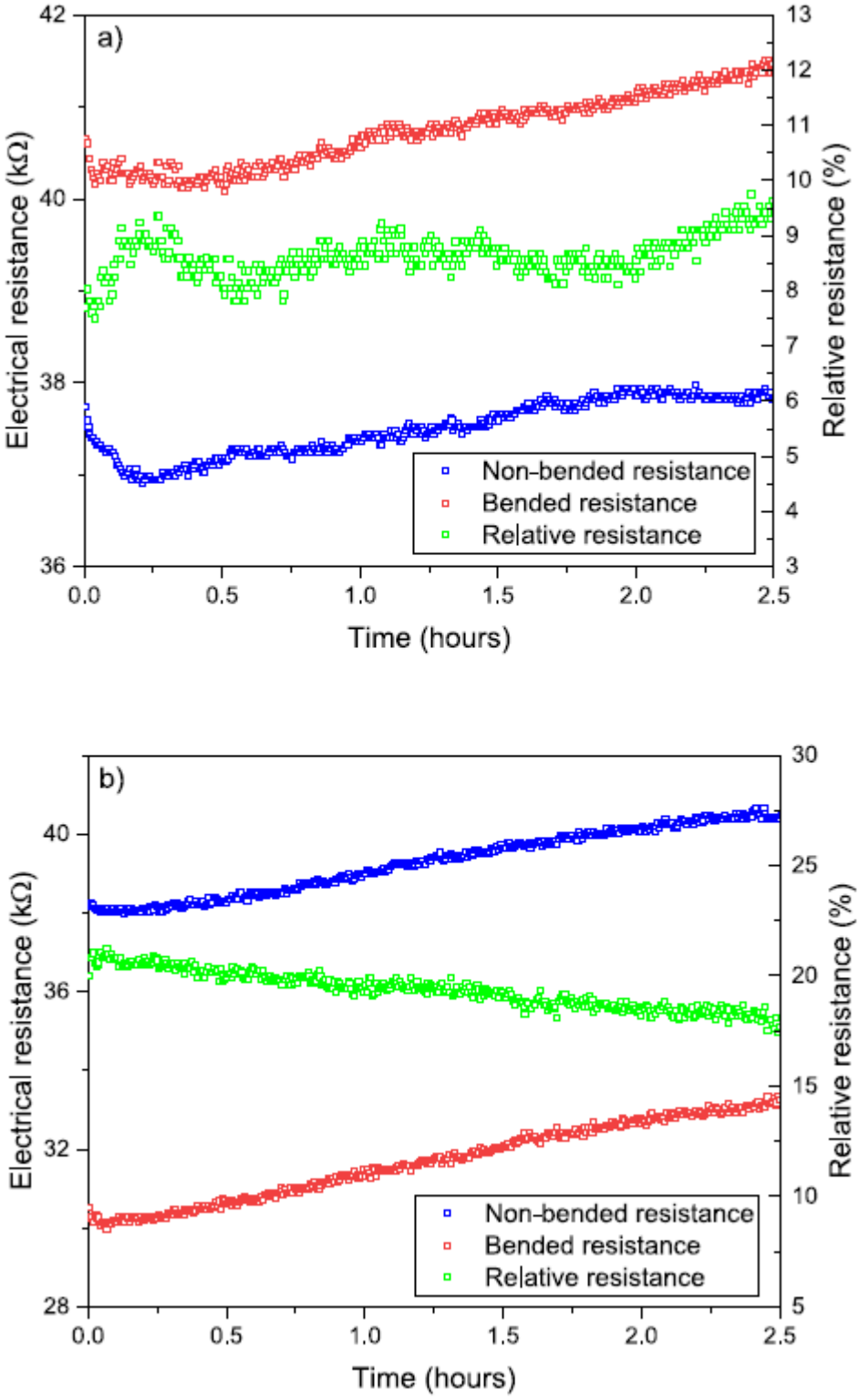

Fig. 9. Cyclic TA/PPy sample bending in (a) the tension and (b) the compression mode.

3.7. Sheet resistence

The original leathers do not display any measurable conductivity. After the coating with PPy, the sheet resistance of all leather was close to each other on both sides, 5—29 kΩ/sq (**Table 3**). The deposition of PPy in colloidal dispersion mode in the presence of HPC led to the increase in the resistance by

about two orders of magnitude, the increase for PVP was less pronounced. It is known that the PPy films deposited on the substrates, here collagen fibers, in the presence of colloidal stabilizers are always thinner than those grown in their absence [**25**]. This is the reason for the higher sheet resistance. In addition, the thickness of conducting layer is smaller in the presence of stabilizers (**Fig. 4**, **Table 1**), which also leads to the sheet higher resistance. This is due to the slower penetration of more viscous reaction mixture containing stabilizers into leather interior.

3.8. Bending tests

Samples of PPy coated leathers were bended 500 times and their DC electrical resistances were compared. A detail of the course of the measured resistance during bending is shown in **Fig. 8**. In the tension mode (**Fig. 8**a), fibers of leather coated by PPy are prolonged and hence electrical resistance is increasing. The response on the sudden angle change is very fast, followed by relaxation of fibers, which is demonstrated as slow decrease and later stabilization of resistance. When bended sample is released, its resistance returns to its original value.

In the pressure mode (**Fig. 8**b), conductive fibers are compressed and hence their electrical resistance is decreasing. The response on sudden angle change is slower than in case of the tension mode and without signal jitter. Relaxation of compressed fibers is demonstrated as slowly falling resistance. The release of the sample leads to the similar course as subjecting the sample to tension. The main difference between the tension and compression mode is in the magnitude of electrical resistance. The magnitude of electrical resistance of compressed sample is always lower than the sample under tension. The angle of bending has also the influence on the magnitude of resistance.

Further trends can be observed from long-term measurements (**Fig. 9**). All leather samples were stiff after in-situ deposition of PPy. Therefore, there is a relatively strong drift of resistances during initial bending cycles due to the sample softening. After ^60 bending cycles (20 min), the stiffness of the sample is stabilized. However, there is a slow drift of resistances toward higher values. According to our opinion, this drift is caused by combination of wear and loosening of the fibers during mechanical stress.

Electrical resistance of both VE/PPy and RA/PPy was one order of magnitude lower. The course of resistance curves was similar to those in the **Fig. 9**, including softening of the sample and slow drifts. However, applying mechanical stress on VE/PPy and RA/PPy leads to low relative resistance changes only, 1.5 % and 5 %, respectively.

4. Conclusions

Polypyrrole-coated leathers were successfully obtained through in-situ oxidative polymerization of pyrrole in absence and presence of poly (N-vinylpyrrolidone) or hydroxypropylcellulose, i.e. in colloidal dispersion mode, using iron(III) chloride as an oxidant. The use of water-soluble polymer stabilizers eliminates the formation of macroscopic adhering polypyrrole precipitate, which produces a “dirty” surface. This was confirmed by scanning electron microscopy. The thickness of the conducting phases was determined by the penetration of reaction mixture into the leather body and was reduced for the coatings performed in the presence of colloidal stabilizers due to higher viscosity of polymer solutions. Optical microscopy demonstrated that the top and bottom coatings were separated with an insulating phase constituted of uncoated collagen fibers. The $FTIR$ and Raman spectroscopies confirmed the complete coating of individual collagen fibers in the conducting phases. The mechanical performance

in terms of break load, tensile strength, and elongation reduced after polypyrrole coating. Electrical properties were represented by sheet resistances in the range of 10^0-10^3 kΩ/sq, with the highest resistance observed for leather coated in the presence of colloidal stabilizers due to the reduced thickness of conducting phase. The changes in the resistance were monitored and demonstrated to decrease in the units of percent after extensive mechanical cycling.

The results observed in this study indicate new possibilities for the use of conducting polymers, e.g., in the footwear industry as antistatic materials that could be heated by the passing current and in the decorative role of polypyrrole coating.

References

[1] D.S. Pramila Devi, P.K. Bipinbal, T. Jabin, K.N. Naranayann Kutty, Enhanced electrical conductivity of polypyrrole/polypyrrole coated short nylon fiber/natural rubber composites prepared by in situ polymerization in latex, Mater. Design 43 (2013) 337-347, **https://doi.org/10.1016/j.matdes.2012.06.042**.

[2] J. Stejskal, Conducting polymers are not just conducting: a perspective for emerging technology, Polym. Int. 69 (2020) 662-664, **https://doi.org/10.1002/ pi.5947**.

[3] P. Humpolíček, V. Kašpárková, J. Pacherník, J. Stejskal, P. Bober, Z. Capáková, K. A. Radaszkiewicz, I. Junkar, M. Lehocký, The biocompatibility of polyaniline and polypyrrole: a comparative study of their cytotoxicity, embryotoxicity and impurity profile, Mater. Sci. Eng. C 91 (2018) 303-310, **https://doi.org/10.1016/). msec.2018.05.037**.

[4] J. Stejskal, M. Trchová, Conducting polypyrrole nanotubes: a review, Chem. Pap. 72 (2018) 1563-1595, **https://doi.org/10.1007/s11696-018-0394-x**.

[5] M.M. Ayad, W.A. Amer, S. Zaghlol, N. Maráková, J. Stejskal, Polypyrrole-coated cotton fabric decorated with silver nanoparticles for the catalytic removal of p-nitrophenol from water, Cellulose 25 (2018) 7393-7407, **https://doi.org/10.1007/ s10570-018-2088-5**.

[6] J. Stejskal, I. Sapurina, J. Vilčáková, M. Jurča, M. Trchová, Z. Kolská, J. Prokeš, I. Křivka, One-pot preparation of conducting melamine/polypyrrole/magnetite ferrosponge, ACS Appl. Polym. Mater. 3 (2021) 1107-1115, **https://doi.org/ 10.1021/acsapm.0c01331**.

[7] T.M. Wu, H.L. Chang, Y.W. Lin, Synthesis and characterization of conductive polypyrrole with improved conductivity and processability, Polym. Int. 58 (2009) 1065-1070, **https://doi.org/10.1002/pi.2634**.

[8] M. Omastová, K. Mosnáčková, M. Trchová, E.N. Konyushenko, J. Stejskal, P. Fedorko, J. Prokes, Polypyrrole and polyaniline prepared with cerium(IV) sulfate oxidant, Synth. Met. 160 (2010) 701-707, **https://doi.org/10.1016/j. synthmet.2010.01.004**.

[9] H.K. Kim, M.S. Kim, S.Y. Chun, Y.H. Park, B.S. Jeon, J.Y. Lee, Y.K. Hong, J. Joo, S. H. Kim, Characteristics of electrically conducting polymer-coated textiles, Mol. Cryst. Liq. Cryst. 405 (2003) 161-169, **https://doi.org/10.1080/ 15421400390263550**.

[10] T. Nezakati, A. Seifalian, A. Tan, A.M. Seifalian, Conductive polymers: opportunities and challenges in biomedical applications, Chem. Rev. 118 (2018) 6766-6843, **https://doi.org/10.1021/acs.chemrev.6b00275**.

[11] I. Gualandi, M. Tessarolo, F. Mariani, L. Possanzini, E. Scavetta, B. Fraboni, Textile chemical sensors based on conductive polymers for the analysis of sweat, Polymers 13 (2021) 894, **https://doi.org/10.3390/polym13060894**.

[12] E.S. Abdel-Halim, S.S. Al-Deyab, Utilization of hydroxypropyl cellulose for green and efficient synthesis of silver nanoparticles, Carbohydr. Polym. 86 (2011) 1615-1622, **https://doi.org/10.1016/j.carbpol.2011.06.072**.

[13] H.Y. Woo, W.G. Jung, D.W. Ihm, J.Y. Kim, Synthesis and dispersion of polypyrrole nanoparticles in polyvinylpyrrolidone emulsion, Synth. Met. 160 (2010) 588-591, **https://doi.org/10.1016/j.synthmet.2009.12.010**.

[14] M. Paúrova, I. Šeděnková, J. Hromádková, M. Babič, Polypyrrole nanoparticles: control of the size and morphology, J. Polym. Res. 27 (2020) 366, **https://doi.org/ 10.1007/s10965-020-02331-x.**

[15] C.M. Ewulonu, J.L. Chukwuneke, I.C. Nwuzor, C.H. Achebe, Fabrication of cellulose nanofiber/polypyrrole/polyvinylpyrrolidone aerogels with Box-Behnken design for optimal electrical conductivity, Carbohydr. Polym. 235 (2020), 116028, **https://doi.org/10.1016/j.carbpol.2020.116028**.

[16] K.M. Koczkur, S. Mourdikoudis, L. Polavarapu, S.E. Skrabalak, Polyvinylpyrrolidone (PVP) in nanoparticle synthesis, Dalton Trans. 44 (2015) 17883-17905, **https://doi.org/10.1039/C5DT02964C**.

[17] F.A. Ngwabebhoh, O. Zandraa, T. Sáha, J. Stejskal, M. Trchová, D. Kopecký, J. Pfleger, J. Prokes, In-situ coating of leather with conducting polyaniline in colloidal dispersion mode, Synth. Met. 291 (2022) 117191, **https://doi.org/ 10.1016/j.synthmet.2022.117191**.

[18] P. Banerjee, S.N. Bhattacharyya, B.M. Mandal, Poly(vinyl methyl ether) stabilized colloidal polyaniline dispersions, Langmuir 11 (1995) 2414-2418, **https://doi.org/ 10.1021/la00007a017**.

[19] A. Riede, M. Helmstedt, V. Riede, J. Stejskal, Polyaniline dispersions. 9. Dynamic light scattering study of particle formation using different stabilizers, Langmuir 14 (1998) 6767-6771, **https://doi.org/10.1021/la980365l**.

[20] S. Maeda, D.B. Cairns, S.P. Armes, New reactive polyelectrolyte stabilizers for polyaniline colloids, Eur. Polym. J. 33 (1997) 245-253, **https://doi.org/10.1016/ S0014-3057(96)00164-4**.

[21] I. Sapurina, A. Riede, J. Stejskal, In-situ polymerized polyaniline films: 3. Film formation, Synth. Met. 123 (2001) 503-507, **https://doi.org/10.1016/S0379-6779 (01)00349-6**.

[22] J. Stejskal, M. Trchová, H. Kasparyan, D. Kopecký, Z. Kolská, J. Prokeš, I. Křivka, J. Vajďák, P. Humpolíček, Pressure-sensitive conducting and antibacterial materials obtained by in situ dispersion coating of macroporous melamine sponges with polypyrrole, ACS Omega 6 (2021) 20895-20901, **https://doi.org/10.1021/ acsomega.1c02330**.

[23] D. Rana, B.M. Mandal, S.N. Bhattacharyya, Miscibility and phase diagrams of poly (phenyl acrylate) and poly(styrene-co-acrylonitrile) blends, Polymer 34 (1993) 1454-1459, **https://doi.org/10.1016/0032-3861(93)90861-4**.

[24] D. Rana, B.M. Mandal, S.N. Bhattacharyya, Analogue calorimetry of polymer blends: poly(styrene-co-acrylonitrile) and poly(phenyl acrylate) or poly(vinyl benzoate), Polymer 37 (1996) 2439-2443, **https://doi.org/10.1016/0032-3861 (96)85356-0**.

[25] A. Riede, M. Helmstedt, I. Sapurina, J. Stejskal, In situ polymerized polyaniline films: 4. Film formation in dispersion polymerization of aniline, J. Colloid Interface Sci. 248 (2002) 413-418, **https://doi.org/10.1006/jcis.2001.8197**.

[26] J. Stejskal, J. Vilčáková, M. Jurča, H.J. Fei, M. Trchová, Z. Kolská, J. Prokeš, I. Křivka, Polypyrrole-coated melamine sponge as a precursor for conducting macroporous nitrogen-containing carbons, Coatings 12 (2022) 324, **https://doi. org/10.3390/coatings12030324**.

[27] J. Stejskal, M. Trchová, P. Bober, Z. Morávková, D. Kopecký, M. Vrňata, J. Prokeš, M. Varga, E. Watzlova, Polypyrrole salts and bases: superior conductivity of nanotubes and their stability towards the loss of conductivity by deprotonation, RSC Adv. 6 (2016) 88382-88391, **https://doi.org/10.1039/C6RA19461C**.